Adsorption and oxidation of carbon monoxide on Au and Ni nanoparticles deposited on Al_2O_3 by laser electrodispersion

T. N. Rostovshchikova,[a] M. I. Shilina,[a] E. V. Golubina,[a] E. S. Lokteva,[a] I. N. Krotova,[a] S. A. Nikolaev,[a] K. I. Maslakov,[a] D. A. Yavsin[b]*

[a]*Department of Chemistry, M. V. Lomonosov Moscow State University, build. 3, 1 Leninskie Gory, 119991 Moscow, Russian Federation. Fax: +7 (495) 932 8846. E-mail: rtn@kinet.chem.msu.ru*
[b]*Ioffe Physical-Technical Institute, Russian Academy of Sciences, 26 ul. Politekhnicheskaya, 194021 Saint Petersburg, Russian Federation. Fax: +7 (812) 297 1017*

Dissociative adsorption of CO on Au and Ni nanoparticles deposited on Al_2O_3 by laser electrodispersion (LED) was for the first time observed using diffuse reflectance infrared Fourier transform (DRIFT) spectroscopy. The average particle size was 4.0 nm for the Au nanoparticles and 1.5—2.0 nm for the Ni nanoparticles. The process on alumina-supported Au nanoparticles of similar size, prepared by ion exchange proceeds with lower efficiency. The Ni/Al_2O_3 catalyst prepared by LED exhibits unusually high activity in the oxidation of CO at $T > 600$ K. When the catalyst was reused, the temperature of CO oxidation decreased to 450 K. The activity of the Au- and Ni-catalysts prepared by LED is higher than that of the catalysts of identical composition prepared by traditional methods, namely, ion exchange and impregnation. The DRIFT and X-ray photoelectron spectroscopy (XPS) data are used to analyze the structure of the catalysts prepared by LED that is associated with specific features of their adsorption and catalytic properties.

Key words: laser electrodispersion, nanoparticles, Au, Ni, oxidation, CO.

Progress in fundamental concepts of heterogeneous catalysis is to a great extent due to the understanding of the mechanism of CO oxidation on the atomic level. The use of modern physicochemical methods for structure elucidation and investigation of the adsorption and oxidation of CO on the surface of thin films and single crystals revealed the role of the interaction between supported metal particles and metal oxides in their catalytic behavior.[1—3] Data on the adsorption and oxidation of CO on model catalysts have been generalized in reviews.[4—6] However, the adsorption of CO on real supported catalysts has been poorly studied as yet. In particular, it is unclear why the catalytic activity of catalysts with close chemical compositions and almost identical particle size depends strongly on the experimental conditions and on the catalyst preparation procedure. More detailed studies of the adsorption of CO require the use of the model catalytic systems that are structurally similar to the real supported systems but have well-specified properties, *e.g.*, the particle size and shape as well as the distribution pattern of particles on the support surface. These requirements are met by nanostructured supported catalysts prepared by laser electrodispersion (LED).[7,8] The method is based on cascade fission of droplets emitted from the surface of a metallic target exposed to high-power laser pulses. Nano-sized droplets produced by fission and deposited on the substrate are rapidly cooled and retain their amorphous state. A feature of the LED method consists in that the size of particles thus prepared is governed by the work function of an electron. Unusually high activity of the catalysts prepared by LED (from this point on, LED-catalysts) is explained as follows.[7—9] First, these catalysts have a narrow size distribution of metal particles, the range of particle sizes being optimum for the highest catalytic activity. Second, the catalysts exhibit high stability toward aggregation and deactivation due to the amorphous state of metal and, probably, to the presence of a thin oxide layer on the surface. Third, the deposition of nanoparticles is accompanied by the formation of a shell on the outer surface of the support. Finally, a high density of contacts between metal particles and the possibility for surface charge fluctuations due to tunneling electronic transitions between neighboring particles as well as between particles and support improve the adsorption and catalytic properties. Laser electrodispersion was used to prepare highly efficient catalysts of hydrodechlorination based on Au and Ni nanoparticles.[10,11] Examples of improved efficiency of the Au catalysts in the presence of Ni in similar processes and in the

Published in Russian in *Izvestiya Akademii Nauk. Seriya Khimicheskaya,* No. 4, pp. 0812—0818, April, 2015.

oxidation of CO have been reported.[12—15] The reasons that cause the bimetallic catalysts to have synergistic properties have been considered in a recent review.[16]

In this work we analyzed specific features of the structure and catalytic behavior of the low-metal mono- and bimetallic Au and Ni catalysts prepared by deposition of Au and Ni on alumina using LED taking the adsorption and oxidation of carbon monoxide as examples. The adsorption of CO on the Au and Ni catalysts was studied by diffuse reflectance infrared Fourier transform (DRIFT) spectroscopy. The results obtained are compared with published data reported for the Au and Ni catalysts prepared by ion exchange and impregnation.[13,15]

Experimental

Granulated γ-Al_2O_3 (180 $m^2\ g^{-1}$, AOK-63-11B, 95%, pellet size 0.4—1 mm, JSC "Angarsk Catalysts and Organic Synthesis Plant") was used. Monometallic catalysts, Au/Al_2O_3 and Ni/Al_2O_3, were prepared by depositing corresponding metal nanoparticles onto Al_2O_3 granules using LED (in the text below, these catalysts are denoted as $Au/Al_2O_3^{LED}$ and $Ni/Al_2O_3^{LED}$, respectively) in a tailor-made cell following a known procedure.[10,11] The $Ni—Au/Al_2O_3^{LED}$ sample was prepared by depositing the Ni nanoparticles onto the freshly prepared Au/Al_2O_3 product while the $Au—Ni/Al_2O_3^{LED}$ sample was prepared by depositing the Au nanoparticles onto the freshly prepared Ni/Al_2O_3 product. The content of supported metals was determined by atomic absorption spectroscopy using a Thermo iCE 3000 spectrometer. Nickel was dissolved following a known procedure;[11] gold-containing samples were treated with Aqua Regia ($HCl : HNO_3 = 4 : 1$) and then with concentrated HF on heating on a water bath (363 K). The bimetallic samples treated with Aqua Regia were dissolved following a known procedure.[11] The LED-catalysts contained 0.01 vt.% of each metal. The Au-containing comparative catalyst, Au/Al_2O_3 (Au content was 0.1 vt.%), was prepared by ion exchange.[17]

DRIFT studies were carried out on a Lumex Sibir Infralum FT-801 Fourier Transform spectrometer equipped with a diffuse reflectance accessory in the range from 900 to 6000 cm^{-1} (resolution 4 cm^{-1}, 128 scans). Catalyst granules or the initial support was placed in a quartz tube with an arm having a CaF_2 optical window and heat treated *in vacuo* at 473 K for 2 h and then at 673 K for an additional 2 h (the pressure was at most 0.01 Pa). Experiments on the adsorption of CO were carried out at 298 K and at CO pressures in the range from 0.08 to 30 kPa. The DRIFT spectra were recorded at room temperature.

X-ray photoelectron spectra of catalysts were recorded on a Kratos Axis Ultra DLD spectrometer using monochromatic Al-Kα radiation (1486.6 eV). Granulated samples and ground powders were fixed in a holder using a two-side adhesive tape. In order to remove the effect of sample charging, the spectra were measured using a neutralizer. The charge compensation conditions were chosen in such a manner that the peak intensities be the highest, the peaks being as narrow as possible. The spectra were recorded at an analyzer transmission energy of 40 eV and an increment of 0.1 eV. The surface area analyzed was about 300×700 μm in size. The energy scale was preliminarily calibrated using the following peaks of standard samples (corresponding metal surfaces were purified by ion sputtering): $Au4f_{5/2}$, 83.96 eV; $Cu2p_{3/2}$, 932.62 eV; and $Ag3d_{5/2}$, 368.21 eV (to an accuracy of ±0.03 eV).

The oxidation of CO was conducted in a fixed-bed quartz tube reactor equipped with a thermocouple in the pulsed mode in the temperature range from 423 to 723 K. The temperature was controlled using an Ursamar-RK42 temperature programming unit. The gas mixture (2 vol.% CO, 1 vol.% O_2, 97 vol.% He) was fed using a six-way valve with a 1 mL chromatographic loop at a pulse repetition rate of 10 pulse h^{-1}. The content of CO and CO_2 in the reaction mixture was analyzed using an LKhM-8MD chromatograph (thermal conductivity detector; a packed column 1 m long, Porapak-Q stationary phase, the temperature of the column was 303 K; the carrier gas (He) flow rate was 30 $cm^3\ min^{-1}$) and the Ecochrom software package for data processing. In all cases, the steady-state conversion attained after 10 to 15 pulses was used to plot the temperature dependences of CO conversion and to compare the catalytic activities of different systems.

Results and Discussion

The structure of catalysts. The morphology of the Ni and Au nanoparticles deposited on Al_2O_3 by LED was studied in detail recently.[10,11] Nickel nanoparticles in the monometallic catalysts are characterized by narrow and unimodal size distributions with an average particle size of about 1.5±0.5 nm. Most of the Au particles in the monometallic samples are larger, being about 4 nm in size, and the particle size range is wider (from 1 to 8 nm). Bimetallic Au—Ni catalysts prepared by LED are characterized by a bimodal size distribution of the metal particles with maxima near 2 and 4 nm, *i.e.*, both particle size distributions characteristic of the monometallic Ni and Au catalysts are reproduced. Local energy-dispersive analysis revealed the presence of both Au and Ni at all analyzed points and regions on the surface of the Au—Ni samples prepared by LED. This suggests a uniform and sufficiently dense coverage of the support surface by both types of metal particles; however, no formation of Au—Ni alloy[10] was detected.

Metal nanoparticles deposited by the LED method have a lower degree of crystallinity compared to nanoparticles prepared by other methods. Support for this suggestion can be found in the absence of the diffraction patterns of fast electrons in the experiments with the freshly prepared LED-samples[7] and in the shape of the metal nanoparticles in high-resolution transmission electron microscopy (HR TEM) images.[10,11] Specific adsorption and catalytic properties of these samples to a great extent originate from amorphous state of the metal.

According to recently published data,[15] the morphology and size of metal particles in the comparative catalysts, *viz.*, supported Au and Ni catalysts (metal content 0.1 mass.%) prepared by ion exchange and impregnation, resemble those of the catalysts prepared by LED. The average size of the Ni- and Au-containing particles in the

monometallic samples was about 3 nm. Particles in the bimetallic samples are somewhat larger, being 4 nm in size.

DRIFT spectra of adsorbed CO. Depending on the surface morphology, method of synthesis, and process conditions, the adsorption of CO on gold surface can be weak, reversible, and lead to the formation of a molecular adsorbate or, more rarely, it can follow a dissociative pathway and afford adsorbed species of carbon and oxygen.[1—4] The strength of adsorption increases as the particle size decreases with the appearance of weakly bound gold atoms.[17] Dissociative adsorption of carbon on the surface of Au(110) thin films was observed at an elevated pressure of CO at 300 K.[2] Therefore, the adsorption of CO is a good test for analysis of the structure of nanosized catalysts.

The DRIFT spectra obtained after the adsorption of CO on the initial γ-Al_2O_3 and on the metal-containing samples prepared by LED at the equilibrium CO pressures in the range from 0.1 to 1.5 kPA are presented in Fig. 1. From Fig. 1 (curves *1*, *3*, *5*) it follows that the adsorption of CO on alumina at 295 K can be observed at elevated pressures only leading to the appearance of a strong absorption band in the region 2200 cm^{-1} and a weak absorption band at 2155 cm^{-1} corresponding to the CO complexes with Lewis acid sites on Al^{3+} and to the H-complexes with weak Brønsted acid sites, respectively.[18] No absorption bands of adsorbed CO were observed in the DRIFT spectrum of Al_2O_3 at pressures lower than 0.2 kPa. At the same time, a weak absorption band at 2206 cm^{-1} corresponding to carbonyl complexes of Ni^{2+} was observed after adsorption of CO on the $Ni/Al_2O_3{}^{LED}$ sample at 0.1 kPa (see curve *6* in Fig. 1).[18] As the CO pressure increases to 1.5 kPa (curves *2* and *4*), the intensity of the band in the region 2200 cm^{-1} increases and its maximum is shifted toward smaller wavenumbers due to the overlap of the absorption bands of the complexes of CO with the Lewis acid sites on alumina (2199 cm^{-1}) and with Ni^{2+} cations (2206 cm^{-1}). Unlike the spectra of the Ni (0.3%)/Al_2O_3 samples prepared by impregnation,[13] the spectra of the samples prepared by LED exhibit no absorption band at 2178 cm^{-1} characteristic of the CO adsorbed on nickel oxide.[18]

Figure 2 presents the DRIFT spectra of CO adsorbed on the surface of samples of different composition at a pressure of 1.5 kPa. A comparison of the spectra in Fig. 2 and spectrum *1* in Fig. 1 shows that the ν(CO) band of carbon monoxide at 2199 cm^{-1} in the complexes with Al^{3+} in the monometallic Ni- and Au-containing samples is weaker than that in the initial Al_2O_3. Considering the DRIFT spectrum of the $Au—Ni/Al_2O_3{}^{LED}$ sample, the band of adsorbed CO is detected only if the equilibrium pressure of CO is ten to fifteen times that of the pressure in the experiments with the initial Al_2O_3 (1.5—2 *vs.* 0.2 kPa, respectively). In other words, at the same equilibrium pressures, the number of adsorbed CO molecules on the surface of γ-Al_2O_3 covered with ultrasmall amounts of Au and/or Ni (at most 0.01 mass %) deposited by LED significantly decreases.

Weakening of the band of the adsorbed CO in the DRIFT spectra of the bimetallic catalyst is accompanied by the appearance of new broad strong bands corresponding to ν(CO) vibrations in the covalently bound carbonate species or weakly adsorbed forms of CO_2 in the range 1800 cm^{-1} (Fig. 3, spectrum *1*).[18] As the CO pressure increases to 24 kPa, the DRIFT spectra of the $Au—Ni/Al_2O_3{}^{LED}$ sample exhibit an increase in the intensity of absorption in the region 1800 cm^{-1} (see spectrum *2* in Fig. 3) and strengthening of the ν(CO) bands at 2100—2200 cm^{-1}. These bands correspond to complexes of CO with the Lewis and Brønsted acid sites of the support as well as physisorbed CO (2199, 2155, and 2130 cm^{-1}, respectively).[18] In Fig. 3 we also compare the spectra recorded immediately after the adsorption of CO (spectrum *2*)

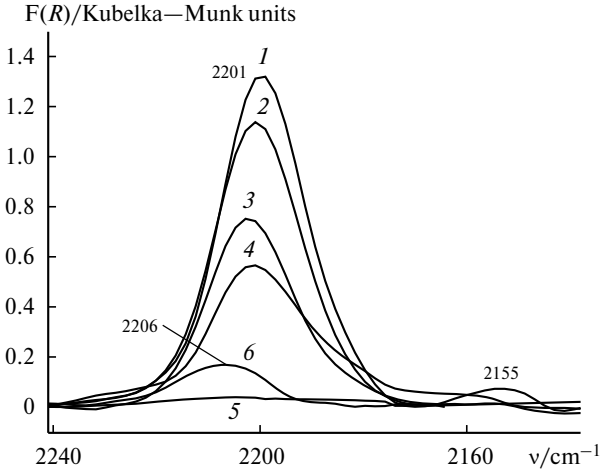

Fig. 1. DRIFT spectra of carbon monoxide adsorbed on Al_2O_3 (*1*, *3*, *5*) and on (0.01% Ni)/$Al_2O_3{}^{LED}$ (*2*, *4*, *6*) at an equilibrium CO pressure of 1.5 (*1, 2*), 0.8 (*3*, *4*), and 0.1 kPa (*5, 6*). T = 295 K.

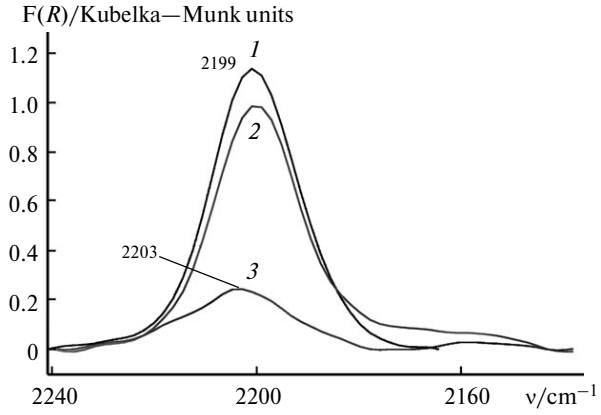

Fig. 2. DRIFT spectra of carbon monoxide adsorbed on $Ni/Al_2O_3{}^{LED}$ (*1*), $Au/Al_2O_3{}^{LED}$ (*2*), and $Au—Ni/Al_2O_3{}^{LED}$ (*3*) at an equilibrium CO pressure of 1.5 kPa and T = 295 K.

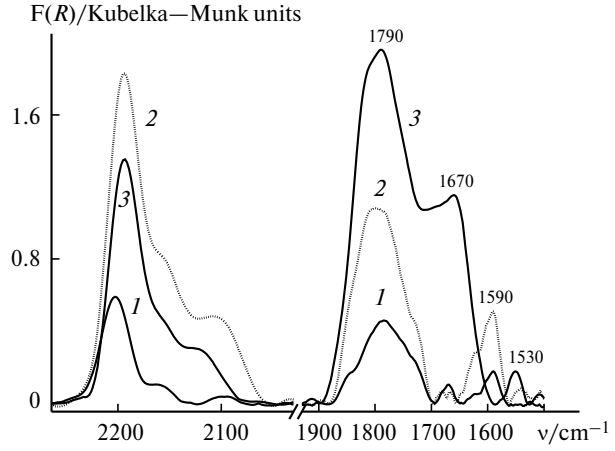

Fig. 3. DRIFT spectra of Au—Ni/$Al_2O_3^{LED}$ sample after adsorption of CO at a pressure of 1.5 (*1*) and 24 kPa (*2*, *3*) recorded immediately after treatment with CO (*2*) and after keeping the sample in CO atmosphere for 24 h at 295 K (*3*).

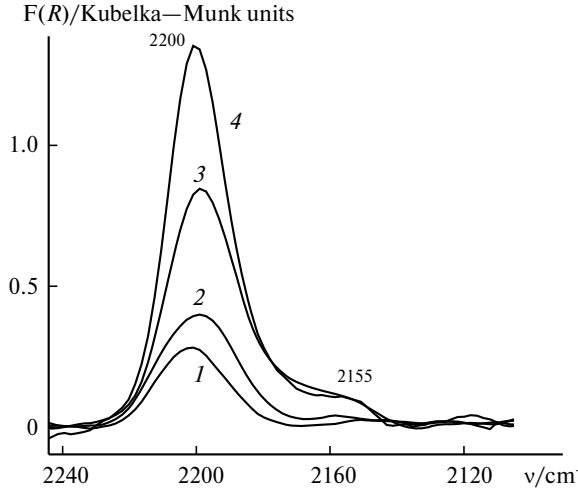

Fig. 4. DRIFT spectra of (0.1% Au)/Al_2O_3 samples prepared by ion exchange (*1*—*3*), and Al_2O_3 (*4*) after adsorption of CO at a pressure of 0.4 (*1*), 1.9 (*2*), and 3.9 kPa (*3*, *4*). T = 295 K.

and after the sample was stored for 24 h in CO atmosphere at 295 K (spectrum *3*). As can be seen, the absorption bands of CO in the region 2100—2200 cm^{-1} become weaker with time, whereas the absorption bands in the region 1500—1800 cm^{-1} become much stronger.

One can assume that chemical transformations of carbon monoxide on the surface of the Au-containing samples prepared by LED occur at room temperature. These processes result in adsorbed CO_2 and carbonate species. Nickel present in the Au—Ni/Al_2O_3 samples in the form of Ni^{2+} cation improves the efficiency of the process and the CO conversion on the surface of bimetallic systems synergistically increases. Thus, the use of CO as a probe molecule to analyze the state of gold atoms on the surface of the nanoparticles deposited by LED revealed an unusual activation of the CO bond.

To elucidate the possibility for similar processes to occur on the classical Au-catalysts prepared by impregnation, the Au(0.1 %)/Al_2O_3 samples prepared by impregnation were tested in analogous conditions. For these samples, room-temperature adsorption of CO on strong Al^{3+} Lewis acid sites of the support (2201 cm^{-1}) was only observed (Fig. 4). As for the LED samples, no absorption bands characteristic of carbon monoxide adsorbed on gold nanoparticles (see, *e.g.*, Refs 2 and 4) were detected in a wide range of the equilibrium pressures of CO (0.1—50 kPa). This can be explained by a low surface concentration of gold; however, the occurrence of chemical processes resulting in irreversible transformation of the probe molecule seems to be more important. This follows from the data in Fig. 4 where the band at 2200 cm^{-1} corresponding to the adsorption of CO on the Al^{3+} sites of the gold-doped support appears to be much weaker than the corresponding band characterizing the adsorption of CO on the initial Al_2O_3 under identical conditions. Most plausibly, the conversion of CO to CO_2 on the low-metal Au/Al_2O_3 samples prepared by ion exchange occurs at room temperature similarly to the process on the LED-samples containing gold nanoparticles of similar size.

The process can follow two pathways, namely, (i) *via* disproportionation of CO to carbon and CO_2 (this was observed on the surface of thin metallic gold films[2]) or (ii) with participation of oxygen from metal oxides.[14] Dissociative adsorption of CO at room temperature is well known; it was studied taking cobalt nanoparticles on magnesium oxide and alumina as examples.[19,20] It is assumed that the process can also occur on gold and platinum clusters on the surface of iron oxides.[21—23] Additional information on the state of metals on the surface of catalysts and on the mechanism of CO formation can be extracted from XPS data.

XPS data for the initial catalysts and after the adsorption of CO. The parameters of the X-ray photoelectron spectra of the low-metal mono- and bimetallic Au- and Ni-catalysts obtained in this work, as well as published data for analogous systems[10,11,13] are presented in Table 1.

It follows that gold on the surface of low-metal LED-catalysts is predominantly in the metallic state, although the presence of tiny Au nanoparticles nearly 4 nm in size or including a small contribution from the charged state, $Au^{\delta+}$, can not be ruled out. At the same time, a small shift of the signal toward higher binding energies can be due to a high degree of dispersion of nanoparticles in the samples. In all cases, nickel is mainly present in the oxidized form and only the LED-catalysts with a metal concentration of higher than 0.01% also contain metallic nickel. According to XPS data, metallic nickel on the surface of the LED-nanoparticles can account for about 40% of the total nickel. The main state, Ni^{2+}, seems to be analogous to the state of nickel in its hydroxide; thus implying the

Table 1. Peak positions in X-ray photoelectron spectra (the spectra were calibrated against the binding energy of the 1*s* electrons of carbon adsorbed on the surface of the samples; the C1s peak energy was taken equal to 285.0 eV) and differences in positions of the $Au4f_{7/2}$, $Ni2p_{3/2}$, and Al2p peaks

Sample	Method	[M] (mass.%)	$Ni2p_{3/2}$	$Au4f_{7/2}$	Al2p	Ni—Al	Au—Al	Reference
			eV					
Ni/Al_2O_3	LED	0.005	856.1	—	74.3	781.8	—	10, 11
	LED	0.03	856.1	—	74.2	781.9	—	11
			853.2	—	—	779.0	—	11
	Impregnation	0.28	855.7	—	74.5	781.2	—	13
Initial	NCD	0.17	855.8	—	74.4	781.4	—	11
Au/Al_2O_3	LED	0.005	—	83.9	74.26	—	9.64	10
	LED	0.01	—	84.37	74.73	—	9.64	—
	IE	0.1	—	84.2	74.6	—	9.60	—
Au/Al_2O_3 after CO	IE	0.1	—	83.9	74.6	—	9.30	—
$Au—Ni/Al_2O_3$	LED	0.01	856.23	84.19	74.33	781.9	9.86	10
$Ni—Au/Al_2O_3$	LED	0.01	856.33	83.99	74.29	782.04	9.70	—

Note. LED is laser electrodispersion of metal, NCD is depositon from nickel colloidal dispersion, IE is ion exchange from alkaline solution of chloroauric acid, Impregnation denotes impregnation from aqueous nickel nitrate.

interaction with the surface hydroxyl groups. The state of nickel is the key difference of these samples from the samples prepared by other methods, *e.g.*, impregnation[13,15] or deposition from colloidal dispersions.[11] These features of the electronic state of nickel in the LED-samples also agree with the DRIFT data considered above.

Since the trends observed in the experiments with the low-content samples prepared by LED and by ion exchange are similar, the influence of the adsorption of CO on the morphology of the catalysts was studied taking $(0.1\%Au)/Al_2O_3$ prepared by ion exchange as an example. The binding energy of $Au4f_{7/2}$ electrons equal to 84.2 eV for the initial sample decreased to 83.9 eV as a result of the adsorption of CO; this corresponds to metallic gold. Carbon monoxide can reduce gold at room temperatures.[24] Since, owing to a large pellet size, the X-ray photoelectron spectra of the granulated catalyst represent almost single-pellet spectra, in order to eliminate the effect of inhomogeneous coverage of granules, we also studied a powder prepared by grinding a few pellets. The ground samples exhibited almost no $Au4f_{7/2}$ XPS spectra.

Figure 5 presents the C1s spectra of the granulated and ground $(0.1\%Au)/Al_2O_3$ samples prepared by ion exchange. The spectra were registered before and after the adsorption of CO. In both cases, the intensity of the C1s peak increases after the adsorption of CO because the content of carbon on the surface increases. This is particularly clearly seen in the spectra of granulated samples. The peak intensities in the spectrum of the ground catalyst also increase upon the adsorption of CO, although to a lesser extent, probably, due to an increase in the total amount of carbon-containing compounds adsorbed on the surface of dispersed samples. However, in this case it is clearly seen that the maximum of the peak undergoes a shift of 0.2 eV toward lower binding energies (E_b); this can be due to the deposition of carbon atoms (E_b = 283.8 eV) on the surface of the catalyst. Similar changes in the C1s spectra during dissociative adsorption of CO in the presence of oxygen were observed in a study of yet another model system, $Au/Fe_2O_3/Fe$.[22]

Carbon monoxide oxidation on the mono- and bimetallic Au- and Ni-catalysts prepared by LED. In Fig. 6, the conversion of CO on the mono- and bimetallic Au and Ni

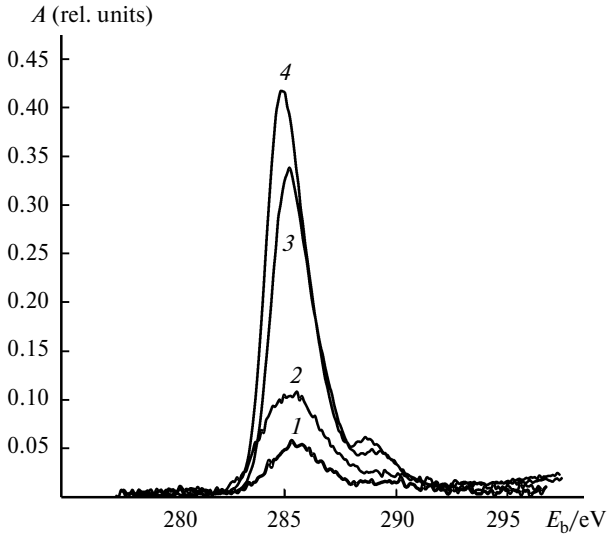

Fig. 5. C1s X-ray photoelectron spectra of $(0.1\%\ Au)/Al_2O_3$ sample prepared by ion exchange: granules before (*1*) and after (*2*) treatment with CO, powder before (*3*) and after (*4*) treatment with CO. The spectra are normalized to the intensity of the Al2p line.

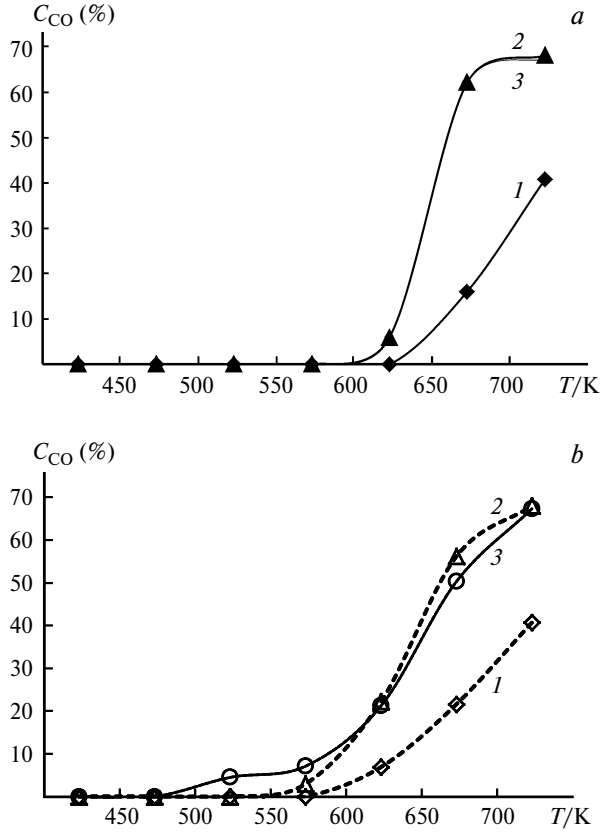

Fig. 6. Carbon monoxide conversion (C_{CO}) on various catalysts plotted *vs.* reaction temperature: $Au/Al_2O_3^{LED}$ (*1*), $Ni/Al_2O_3^{LED}$ (*2*), and $Ni—Au/Al_2O_3^{LED}$ (*3*). The curves were obtained in the heating (*a*) and cooling (*b*) modes.

catalysts prepared by LED is plotted *vs.* temperature under conditions of successive stepwise increase and subsequent decrease in the reaction temperature. As can be seen, the oxidation of CO occurs at a high rate only at relatively high temperatures (above 573 K), namely, a 10% conversion of CO on $Au/Al_2O_3^{LED}$ and $Ni/Al_2O_3^{LED}$ is achieved at 651 and 627 K, respectively. The activity of the catalyst based on Ni nanoparticles is higher than that of the Au-containing analogue. Based on the published data, one could expect a higher activity of the gold-containing catalysts compared to that of nickel oxide because, *e.g.*, the activity of gold and nickel oxide at 573 K is 15 and 0.013 arbitrary units, respectively.[6] A similar order of activities was also observed for the conventionally supported catalysts Au/Al_2O_3 and Ni/Al_2O_3 prepared by ion exchange and impregnation. In this case, the nickel-containing catalyst in which most part of nickel is present in the form of nickel oxide, is inactive in the oxidation of CO.[15] This is probably due to the fact that nickel present in the LED-prepared Ni nanoparticles active in the oxidation exists in two electronic states, *viz.*, Ni^{2+} and Ni^0 even on the surface of alumina. Heterogeneous composition of the LED-deposited Ni nanoparticles containing metallic-conductivity and zero-conductivity regions corresponding to (probably) nonstoichiometric nickel oxides was demonstrated recently by scanning tunneling spectroscopy (STS).[25] Probably, the enhanced activity of nickel nanoparticles is due to the different electronic states of nickel and to other specific features of the nanoparticles deposited by LED, such as accessibility of the active phase, amorphous state of nanoparticles, the possibility for charge interactions to occur, *etc.*[7—11]

The $(0.01\%Au)/Al_2O_3^{LED}$ catalysts are much more active than the $(0.1\%Au)/Al_2O_3$ catalysts prepared by ion exchange. A 10% conversion on the ion-exchange samples is achieved at 680 K, which is 30 K higher than on the LED catalysts.[15] Although the content of metals in the catalysts prepared by LED and by ion exchange differs by an order of magnitude, the catalysts contain mainly metallic gold nanoparticles of similar size and composition. The differences in their catalytic activities are not as high as those shown by the nickel catalysts. Probably, these differences are due to specific features of the structure of the nanoparticles prepared by LED, first of all, their amorphous state and accessibility of the active phase.

From Fig. 6 it follows that the $Ni—Au/Al_2O_3^{LED}$ catalysts are comparable in activity with the $Ni/Al_2O_3^{LED}$ catalysts. This differs the bimetallic systems prepared by LED from the classical bimetallic catalysts that are characterized by synergistic enhancement of activity compared to that of the monometallic analogues. This can be explained by the character of formation of bimetallic nanoparticles during successive deposition of components and by appearance of new active sites at the metal—oxide interface.[15] Bimetallic LED-catalysts exhibit enhanced activity only when re-used at lower temperatures.

From the data in Fig. 6 it follows that activity plots measured on lowering the reaction temperature yield higher conversions of CO on $Ni—Au/Al_2O_3^{LED}$ at $T < 623$ K than those achieved at the same temperatures in the heating mode. The operating range for the bimetallic catalyst extends itself by almost 150 K toward lower temperatures. For the whole temperature range studied, the conversion of CO on the $Au/Al_2O_3^{LED}$ catalyst measured in the cooling mode is also somewhat higher than that determined in the heating mode; in this case, the operating range of the catalyst is extended by 50 K toward lower temperatures. One can assume that improved performance of the catalysts upon heating is due to the fact that the dissociation of CO occurs at room temperature and most probably leads to deactivation of the catalyst owing to coke formation. When the catalysts operate at elevated temperatures under oxidative conditions, their activity increases due to carbon burning; this is particularly pronounced in the cooling mode. We found that the dissociation of CO occurs most efficiently on the surface of gold in the $Ni—Au/Al_2O_3^{LED}$ samples. Probably, it is the coke formation that "switches

on" the activity of gold in the bimetallic LED-catalysts only upon heating of the catalysts.

Summing up, in this work the possibility for dissociative adsorption of CO on the surface of gold nanoparticles to occur at room temperature under anaerobic conditions was demonstrated for the first time using DRIFT spectroscopy and XPS. We found that the process is particularly efficient when using the $Ni—Au/Al_2O_3^{LED}$ catalysts. Specific adsorption properties of the LED-deposited Au and Ni nanoparticles toward hydrogen, oxygen, and nitrogen were observed recently when analyzing such particles by scanning tunneling microscopy and STS.[25,26] One can state that nanostructured metal films deposited by LED differ in structure and properties from the catalysts prepared by the classical methods and containing size-selected metal nanoparticles. A deeper insight into the reasons for these distinctions will favor the development of novel method for improving the efficiency of nanocatalysis.

This work was financially supported by the Russian Science Foundation (Project No. 14-13-00574). The authors acknowledge partial support from the M. V. Lomonosov Moscow State University Program of Development.

References

1. H.-J. Freund, G. Meijer, M. Scheffler, R. Schlögl, M. Wolf, *Angew. Chem. Int. Ed. Engl.*, 2011, **50**, 10064.
2. Y. Jugnet, F. J. Cadete Santos Aires, C. Deranlot, L. Piccolo, J. C. Bertolini, *Surf. Sci.*, 2002, **521**, L639.
3. T. Risse, Sh. K. Shaikhutdinov, N. Nillius, M. Sterrer, H.-J. Freund, *Acc. Chem. Res.*, 2008, **41**, 949.
4. R. Meyer, C. Lemire, Sh. K. Shaikhutdinov, H.-J. Freund, *Gold Bull.*, 2004, **37**, 72.
5. J. Mizera, N. Spiridis, R. P. Socha, M. Zimowska, R. Grabowski, K. Samson, J. Korecki, *Catalysts*, 2012, **2**, 38.
6. S. Royer, D. Duprez, *ChemCatChem*, 2011, **3**, 24.
7. T. N. Rostovshchikova, V. V. Smirnov, V. M. Kozhevin, D. A. Yavsin, S. A. Gurevich, *Nanotechnologies in Russia* (*Engl. Transl.*), 2007 [*Rossiiskie nanotekhnologii*, 2007, **2**, 47].
8. T. N. Rostovshchikova, S. A. Nikolaev, E. S. Lokteva, S. A. Gurevich, V. M. Kozhevin, D. A. Yavsin, A. V. Ankudinov, *Stud. Surf. Sci. Catal.*, 2010, **175**, 263.
9. T. N. Rostovshchikova, E. S. Lokteva, N. E. Kavalerskaya, S. A. Gurevich, V. M. Kozhevin, D. A. Yavsin, *Theor. Exp. Chem.* (*Engl. Transl.*), 2013, **49**, 40 [*Teoret. Eksperim. Khimiya*, 2013, **49**, 37].
10. E. S. Lokteva, A. A. Peristyy, N. E. Kavalerskaya, E. V. Golubina, L. V. Yashina, T. N. Rostovshchikova, S. A. Gurevich, V. M. Kozhevin, D. A. Yavsin, V. V. Lunin, *Pure Appl. Chem.*, 2012, **84**, 495.
11. N. E. Kavalerskaya, E. S. Lokteva, T. N. Rostovshchikova, E. V. Golubina, K. I. Maslakov, *Kinet. Catal.* (*Engl. Transl.*), 2013, **54**, 597 [*Kinet. Katal.*, 2013, **54**, 631].
12. M. A. Keane, S. Gómez-Quero, F. Cárdenas-Lizana, W. Shen, *ChemCatChem*, 2009, **1**, 270.
13. O. P. Tkachenko, L. M. Kustov, S. A. Nikolaev, V. V. Smirnov, K. V. Klementiev, A. V. Naumkin, I. O. Volkov, A. Yu. Vasilkov, D. Yu. Murzin, *Top. Catal.*, 2009, **52**, 344.
14. J. Knudsen, L. R. Merte, G. Peng, R. T. Vang, A. Resta, E. Lægsgaard, J. N. Andersen, M. Mavrikakis, F. Besenbacher, *ACSNano*, 2010, **4**, 4380.
15. S. A. Nikolaev, E. V. Golubina, L. M. Kustov, A. L. Tarasov, O. P. Tkachenko, *Kinet. Catal.* (*Engl. Transl.*), 2014, **55**, 311 [*Kinet. Katal.*, 2014, **55**, 326].
16. O. G. Ellert, M. V. Tsodikov, S. A. Nikolaev, V. M. Novotortsev, *Russ. Chem. Rev.* (*Engl. Transl.*), 2014, **83**, 718 [*Usp. Khim.*, 2014, **83**, 718].
17. C. Lemire, R. Meyer, Sh. K. Shaikhutdinov, H.-J. Freund, *Surf. Sci.*, 2004, **552**, 27.
18. A. A. Davydov, *Molecular Spectroscopy of Oxide Catalyst Surfaces*, Ed. N. T. Sheppard, Wiley, 2003, 684 pp.
19. J. Couble, D. Bianchi, *Appl. Catal. A: General*, 2012, **445**—**446**, 1.
20. K. Mohana Rao, D. Scarano, G. Spoto, A. Zecchina, *Surf. Sci.*, 1988, **204**, 319.
21. Y. Iizuka, H. Fujiki, N. Yamauchi, T. Chijiwa, S. Arai, S. Tsubota, M. Haruta, *Catal. Today*, 1997, **36**, 115.
22. A. F. Carley, D. J. Morgan, N. Song, M. W. Roberts, S. H. Taylor, J. K. Bartley, D. J. Willock, K. L. Howard, G. J. Hutchings, *Phys. Chem. Chem. Phys.*, 2011, **13**, 2528.
23. Y.-N. Sun, Z.-H. Qin, M. Lewandowski, S. Shaikhutdinov, H.-J. Freund, *Surf. Sci.*, 2009, **603**, 3099.
24. K. Chakarova, M. Mihaylov, S. Ivanova, M. A. Centeno, K. Hadjiivanov, *J. Phys. Chem. C*, 2011, **115**, 21273.
25. M. V. Grishin, A. K. Gatin, N. V. Dokhlikova, A. A. Kirsankin, V. A. Kharitonov, B. R. Shub, *Russ. Chem. Bull.* (*Int. Ed.*), 2013, **62**, 1525 [*Izv. Akad. Nauk. Ser. Khim.*, 2013, **62**, 1525].
26. A. K. Gatin, M. V. Grishin, S. A. Gurevich, N. V. Dokhlikova, A. A. Kirsankin, V. M. Kozhevin, N. N. Kolchenko, T. N. Rostovshchikova, V. A. Kharitonov, B. R. Shub, D. A. Yavsin, *Russ. Chem. Bull.* (*Int. Ed.*), 2014, **63**, 1696 [*Izv. Akad. Nauk. Ser. Khim.*, 2014, **63**, 1696].

Received October 31, 2014